

## CLASSIFICATION OF WELD DEFECTS BASED ON CONVOLUTION NEURAL NETWORK

A.I. Gavrilov

alexgavrilov@bmstu.ru

M.Tr. Do

dominhtrieuvhp@gmail.com

**Bauman Moscow State Technical University, Moscow, Russian Federation**

---

### Abstract

Automatic welding technology has been widely applied in many industrial fields. It is a complex process with many nonlinear parameters and noise factors affecting weld quality. Therefore, it is necessary to inspect and evaluate the quality of the weld seam during welding process. However, in practice there are many types of welding seam defects, causes and the method of corrections are also different. Therefore, welding seam defects need to be classified to determine the optimal solution for the control process with the best quality. Previously, the welder used his experience to classify visually, or some studies proposed visual classification with image processing algorithms and machine learning. However, it requires a lot of time and accuracy is not high. The paper proposes a convolutional neural network structure to classify images of welding seam defects from automatic welding machines on pipes. Based on comparison with the classification results of some deep machine learning networks such as VGG16, Alexnet, Resnet-50, it shows that the classification accuracy is 99.46 %. Experimental results show that the structure of convolutional neural network is proposed to classify images of weld seam defects have availability and applicability

### Keywords

*Welding defect classification,  
convolution neural network*

Received 13.02.2020

Accepted 12.12.2020

© Author(s), 2021

---

**Introduction.** Nowadays, with the strong development of science and technology, automatic welding technology is increasingly widely used in many fields such as nuclear, aerospace, chemical, machine design, energy generation, shipbuilding, petrochemical engineering, and other industries [1]. Welding is a complex nonlinear process, which is often affected by welding parameters and environmental uncertainty. Therefore, it is easy to form weld seam defects such as overlap, pore, spatter, slag inclusion, and incomplete fusion. These de-

fects, if not detected during welding, will endanger the durability and reliability of the parts and structure. Therefore, their detection, identification, inspection and classification are very important. There are two methods of weld seam quality inspection and evaluation as Non Destructive Testing (NDT) and Destructive Testing (DT). The objective is to determine the strength of the weld seam by several types of load tests [2]. NDT is a method of inspecting the surface of weld seam to detect defects without harming people and materials, while DT is the inspection by breaking weld seam. Frequently used non-destructive inspecting methods include ultrasonic testing [3], ray detection [4] and eddy current testing [5]. However, they all have disadvantages such as: ultrasound testing is limited by changes in direction, location, shape of defects, ray detection is easy to affect the human body, eddy current testing can only be applicable to materials that generate eddy currents.

In recent decades, computer vision has become an important part of artificial intelligence, which is widely used in the detection, identification and classification of weld defects [6]. This process includes the following main stages: image acquisition, image preprocessing, feature extraction and classification. Feature extraction is one of the most important tasks. Many studies were published in the problem of feature extraction and welding seam defect classification. Yan, et al. [7] has located and segmented welded seam defects by multiple thresholds method and used Support Vector Machine (SVM) to classify defect and non-defect features. Valavanis, et al. [8] extracted geometric features and texture measurements using image processing algorithms such as Local thresholding with Sauvola, morphological filtering to remove single dot, graph-based segmentation algorithms to include in classifiers such as Support Vector Machine, Neural Network, k-NN. Boaretto, et al. [9] extracted defects by the exposure technique of Double Wall Double Image (DWDI) and used Multi-Layer Perception (MLP) to classify continuous the type of defect and non-defect. Zapata, et al. [10] extracted 12 geometric features and directions by image processing techniques, including noise reduction, contrast enhancement, thresholding, and labeling and welding seam defect identification; then proposed a competition between an Artificial neural Network (ANN) and an Adaptive-Network-based Fuzzy Inference System (ANFIS) for weld defect classification. Jiang, et al. [11] proposed a method based on texture features and Principal Component Analysis (PCA) to extract features and use multiclass Support Vector Machine (SVM) to classify weld defects.

However, the above features extraction and classification methods only utilize texture or geometric features of the weld defects images, they ignored many high-level features to distinguish images.

Deep Learning, as a branch of Machine Learning, employs algorithms to process data and imitate the thinking process. The history of Deep Learning can be traced back to 1943, when Walter Pitts and Warren McCulloch created a computer model based on the neural networks of the human brain. Since then, a lot of research on various neural network models has been launched. However, due to the disappearance of gradient in the training methods, it is difficult to create a strong model. The problem was solved with the appearance of deep learning methods by Krizhevsky, et al. [12] built a convolution neural network called Alexnet to classify 1.2 million high-resolution images in the ImageNet LSVRC-2010 contest, boosting the development prospects of deep learning. Later, many researchers announced popular models such as VGGNet, ZFNet, GoogLeNet, Resnet, VGG16, VGG19 and inceptionv3 used to classify large-scale images. The advantage of these methods over traditional methods is no need to perform image preprocessing to extract features. They are capable of learning high-level features from sampling by supervised learning [13].

Recently, several researchers have used deep learning methods to detect and classify welding defects. Sizyakin, et al. [14] proposed a combination of convolutional neural networks and support vector machine to detect four types of welding defects including non-welded, foreign inclusions, cracks, pores. Zhu, et al. [15] built a convolutional neural networks structure to extract high-level features after performing some image preprocessing algorithms, using random forest algorithms to predict the results of welding defect classification. Hou, et al. [16] used convolutional neural network structure with softmax classification combined with a validation threshold to detect weld defects based on X-RAY image data set from [17]. Hou, et al. [18] used SSAE (Stacked Sparse Auto-Encoders) and Deep Convolutional Neural Network (DCNN) models to extract high-level features from the X-RAY dataset of the weld defect, then used a softmax classification types to classify them. Yang, et al. [19] proposed an improved convolutional neural network structure in the activation function of convolution layer “LReLU + Softplus” to classify X-RAY images of welding defects, better results than traditional classification methods. Liu, et al. [20] proposed an improved VGG16 structure based on fully convolutional structure, the model can use input data sets with 2 different sizes of  $256 \times 256$  and  $128 \times 128$  simultaneously when performing the accuracy test of the model. Golodov, et al. [21] combined FgSegNet convolutional neural network structure and traditional CNN network to perform welding defect segmentation and detection from X-RAY images dataset. Khumaidi, et al. [22] used the Gaussian Kernel in each convolution layer to increase the ability

to blur images and eliminate noise, helping the features extraction process to not lose information, increasing classification accuracy.

This paper structure is as follows: types of welding defects in the first part, proposed convolution neural network architecture are discussed in the second Part, experiments and results are discussed in the third part, conclusions are summarized in the last part.

**Types of welding defects.** During welding, weld defects are often caused by many different reasons such as: inappropriate welding technique, welding parameters errors, protective gas conditions, dirty welding materials, welding angles errors, etc. There are many types of weld seam surface defects. However, there are basically six main types of defects: crack, porosity, undercut, incomplete fusion, slag inclusions, spatter described in Fig. 1.

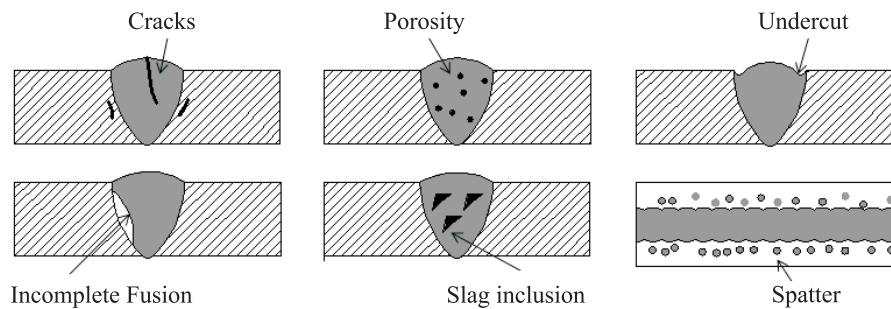


**Fig. 1.** Basic types of welding defects

**Crack.** The most serious type of welding defect is a weld crack and it's not accepted almost by all standards in the industry. It can appear on the surface, in the weld metal or the area affected by the intense heat. There are different types of cracks, depending on the temperature at which they occur.

*Hot cracks* can occur during the welding process or during the crystallization process of the weld joint. The temperature at this point can rise over 10 000 °C.

*Cold cracks* appear after the weld has been completed and the temperature of the metal has gone down. They can form hours or even days after welding. It mostly happens when welding steel. The cause of this defect is usually deformities in the structure of steel.

*Crater cracks* occur at the end of the welding process before the operator finishes a pass on the weld joint. They usually form near the end of the weld. When the weld pool cools and solidifies, it needs to have enough volume to overcome shrinkage of the weld metal. Otherwise, it will form a crater crack.

Causes of this defect include: use of hydrogen when welding ferrous metals, residual stress caused by the solidification shrinkage, base metal contami-

nation, high welding speed but low current, no preheat before starting welding, poor joint design, a high content of sulfur and carbon in the metal.

**Porosity.** Porosity occurs as a result of weld metal contamination. The trapped gases create a bubble-filled weld that becomes weak and can with time collapse. The cause by: inadequate electrode deoxidant, using a longer arc, the presence of moisture, improper gas shield, incorrect surface treatment, use of too high gas flow.

**Undercut.** This welding imperfection is the groove formation at the weld toe, reducing the cross-sectional thickness of the base metal. The result is the weakened weld and workpiece. The cause by: too high weld current, too fast weld speed, the use of an incorrect angle, which will direct more heat to free edges, the electrode is too large, incorrect usage of gas shielding, incorrect filler metal and poor weld technique.

**Incomplete fusion.** This type of welding defect occurs when there's a lack of proper fusion between the base metal and the weld metal. It can also appear between adjoining weld beads. This creates a gap in the joint that is not filled with molten metal. It is caused by the following reasons: low heat input, surface contamination, electrode angle is incorrect, the electrode diameter is incorrect for the material thickness you're welding, travel speed is too fast and the weld pool is too large and it runs ahead of the arc.

**Slag inclusions.** This type of welding defect appears on the surface of the weld seam in the form of large welding slag distribution, has low cohesion and especially poor aesthetics. It is caused by such reasons as: large welding current, high welding speed, high welding electrode supply speed.

**Spatter.** Spatter occurs when small particles from the weld attach themselves to the surrounding surface. It's an especially common occurrence in gas metal arc welding. No matter how hard you try, it can't be completely eliminated. However, there are a few ways you can keep it to a minimum. It is caused by the following reasons: the running amperage is too high, voltage setting is too low, the work angle of the electrode is too steep, the surface is contaminated, the arc is too long, incorrect polarity and erratic wire feeding.

**CNN architecture.** The convolution neural network architecture used to detect and classify three defects and one no-defect is depicted in Fig. 2. It has 29 layers, including: input image layer ( $120 \times 80 \times 1$ ), six convolution layers (C1–C6), five layers of Average-Pooling (S1–S5), between the convolution and Average-Pooling layers there are the batchNormalization and Rectified Linear Unit (ReLU) layers, dropoutLayer layer, two layers FullyConnected FC1–FC2, softmax layer and Classification layer.

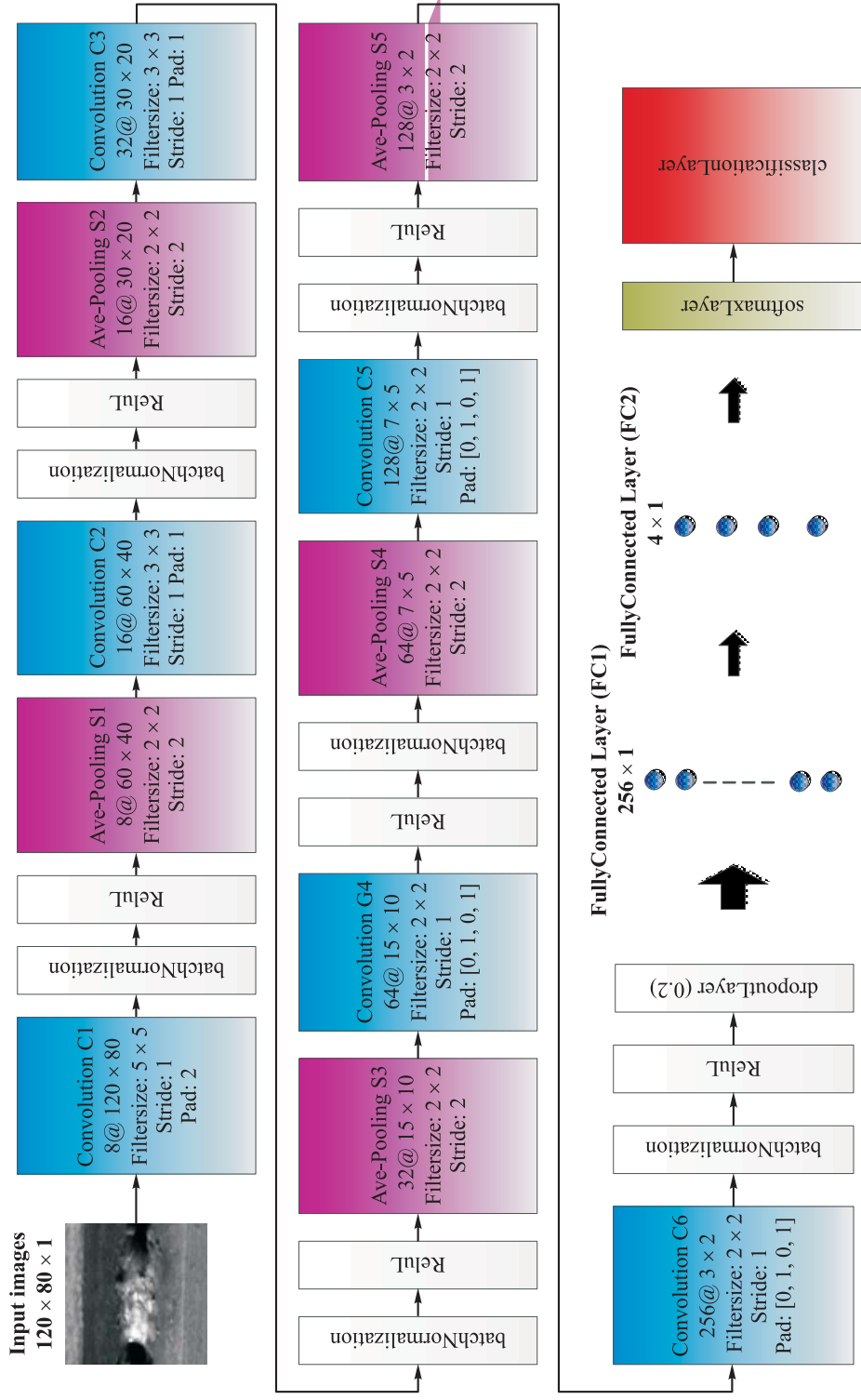


Fig. 2. The convolution neural network architecture is used to train the welding defect classification model

**Convolution layer.** A convolution layer is a fundamental component of the CNN architecture that performs feature extraction. Convolution is a specialized type of linear operation used for feature extraction, where a small array of numbers, called a kernel, is applied across the input, which is an array of numbers, called a tensor. An element-wise product between each element of the kernel and the input tensor is calculated at each location of the tensor and summed to obtain the output value in the corresponding position of the output tensor, called a feature map.

At the initial stage of the training process, the kernels matrix is set by random values. Then extract the features map of the input image by convolution of the image matrix with the kernels matrix. The convolution operation in the paper is determined by the following expression:

$$X_{w,h}^l = f \left( \text{BN} \left( \sum_w \sum_h X_{w+m,h+n}^{l-1} K_{w,h}^l + b \right) \right), \quad (1)$$

where  $X_{w,h}^l$  is the feature map of layer  $l$ ;  $K_{w,h}^l$  is the convolution kernel; BN is the Batch normalization function to normalize the data of feature map,  $f$  is the activation function of the hidden layer;  $X_{w+m,h+n}^{l-1}$  is feature map of the previous layer and  $b$  is bias.

Before using the activation function, the data of feature map is normalized to speed up training of convolutional neural networks and reduce the sensitivity to network initialization. A batch normalization normalizes its inputs  $x_i$  by first calculating the mean  $\mu_B$  and variance  $\sigma_B^2$  over a mini-batch and over each input channel. It calculates the normalized activations as

$$\hat{x}_i = \frac{x_i - \mu_B}{\sqrt{\sigma_B^2 + \varepsilon}}. \quad (2)$$

Here  $\varepsilon$  improves numerical stability when the mini-batch variance is very small. To allow for the possibility that inputs with zero mean and unit variance are not optimal for the layer that follows the batch normalization layer, the batch normalization layer further shifts and scales the activations as

$$y_i = \gamma \hat{x}_i + \beta. \quad (3)$$

With the offset  $\beta$  and scale factor  $\gamma$  are learnable parameters that are updated during network training.

A rectified linear unit (ReLU) is used as the activation function in hidden layers:

$$f(x) = \max(0, x), \quad (4)$$

where  $x$  is the output value of the batch normalization layer.

**Average Pooling Layer.** A pooling layer provides a typical downsampling operation which reduces the in-plane dimensionality of the feature maps in order to introduce a translation invariance to small shifts and distortions, and decrease the number of subsequent learnable parameters. Max Pooling, Global average pooling or Average Pooling can be used depending on network structure and parameters. Average Pooling is used in this research to perform down-sampling by dividing the input into rectangular pooling regions and computing the average values of each region. The average pooling operation is calculated as

$$f_{ave}(x) = \frac{1}{V} \sum_1^V x_i, \quad (5)$$

where the vector  $x$  contains activation values from a local pooling region of  $V$  pixels (pooling region dimensions are  $2 \times 2$ ) in an image or a channel.

**Dropout layer (0.2).** The layer randomly sets input elements to zero given by the dropout mask  $\text{rand}(\text{size}(x))$  less than 0.2, where  $x$  is the layer input and then scales the remaining elements by 1.25. This operation effectively changes the underlying network architecture between iterations and helps prevent the network from overfitting.

**Fully Connected Layer.** The output feature maps of the final convolution and dropout layer is typically flattened, transformed into a one-dimensional (1D) array of numbers, and connected to two fully connected layers FC1 and FC2, in which every input is connected to every output by a learnable weight. Once the features extracted by the convolution layers and downsampled by the pooling layers are created, they are mapped by a subset of fully connected layers to the probabilities for each weld defect and non-defect in classification tasks. The final fully connected layer (FC2) has four output nodes as the number of weld defect and non-defect. Each fully connected layer is followed by a nonlinear function, such as Softmax function, as described in architecture.

**Softmax layer.** Softmax layer applies a softmax function to the input. The softmax function also known as normalized exponential function is the output unit activation function of final fully connected layer, described as:

$$y_r(x) = \frac{\exp(a_r(x))}{\sum_{j=1}^k \exp(a_j(x))}, \quad (6)$$



where  $0 \leq y_r \leq 1$  and  $\sum_{j=1}^k y_j = 1$ ;  $a_r(x)$  is the conditional probability of the sample given class  $r$ , vector  $x$ ;  $j = 1 : k$  is the number of classification classes.

**Classification layer.** Classification layer computes the cross entropy loss for four class classification with mutually exclusive classes. The input of this layer is the output of the softmax layer. Training process in classification layer will takes the values from the softmax function and assigns each input to one of the  $K$  mutually exclusive classes using the cross entropy function described as:

$$\begin{aligned} \text{loss}(y(x), y_r(x)) &= \\ &= -\frac{1}{N} \sum_{x=1}^N [y(x) \log(y_r(x)) + (1 - y(x)) \log(1 - y_r(x))], \end{aligned} \quad (7)$$

where  $N$  is the number of samples;  $y_r(x)$  is the label predicted by our classifier (output of softmax layer);  $y(x)$  — ground truth label.

**Training Optimization Algorithm.** Stochastic gradient descent with momentum (SGDM) is used to optimize and updated training parameters. They are updated according to the following formula:

$$\theta_{l+1} = \theta_{l-\alpha} \nabla E(\theta_l) + \gamma(\theta_l - \theta_{l-1}), \quad (8)$$

where  $\theta_{l+1}$ ,  $\theta_l$ ,  $\theta_{l-1}$  are parameters of next, current and previous iteration step;  $\alpha$  is learning rate;  $\gamma$  is momentum term, determines the contribution of the previous gradient step to the current iteration,  $\gamma = 0.8$ .

**Experiments and results.** An image data set of three weld defects and one non-defect was collected at the “Welding and Control” Center, Bauman Moscow State Technical University, Moscow, Russian Federation. After performing a number of image processing operations such as resizing and defect segmentation, obtained a data set of 6000 images for each type in Fig. 3. Each image is sized to  $120 \times 80$  in RGB format. Each type is selected and labeled based on the experience of the welder, observing the structure, the shape of the weld seam surface. The data set is divided into three parts: 60 % training data, 20 % validation data and 20 % test data. Training results are described in Fig. 4.

The training takes place in 30 epochs, 7410 iterations, initial learning rate of 0.001, running in single CPU mode for a period of 131 minutes. The training process has an accuracy of 99.62 %. The accuracy and error of the training process are demonstrated in Fig. 5.

After training the model, the test data set is used to check the classification accuracy and error of the proposed model. It is a set of 4800 images of four types of welding defect and non-defect taken at random 20 % of the original data set.

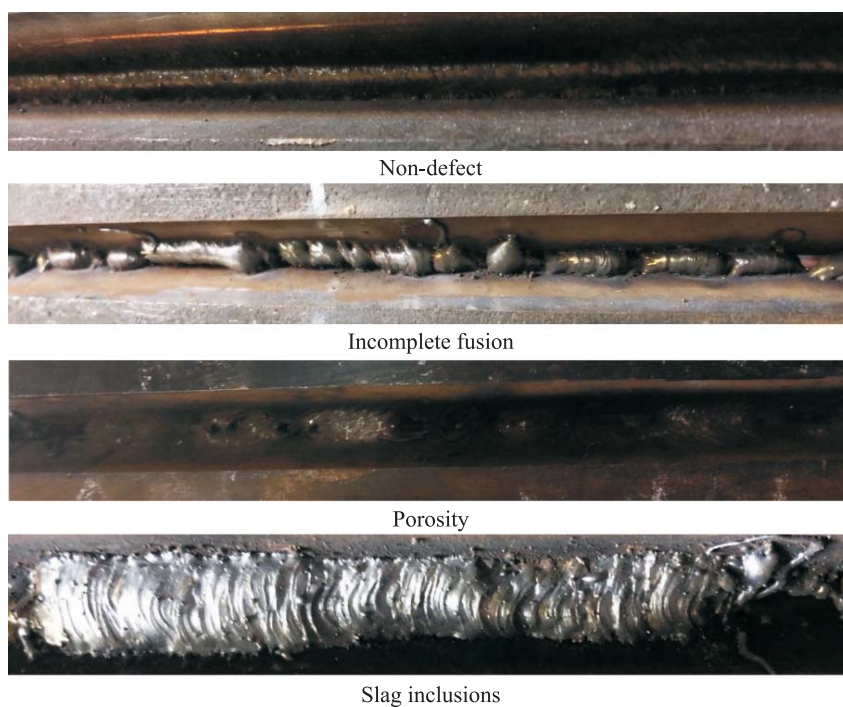


**Fig. 3.** Image of four types of welding defect and non-defect used to train classification model

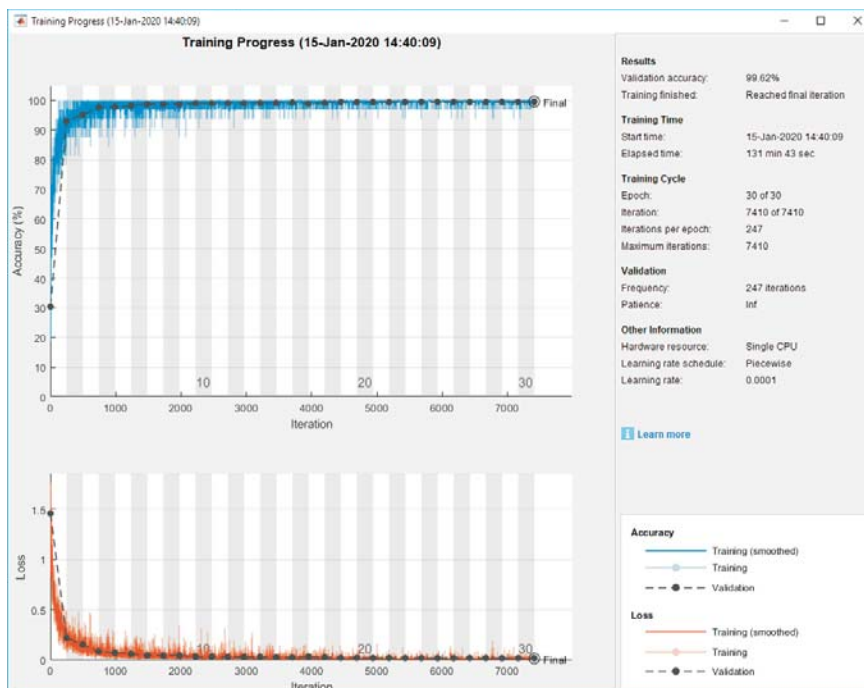


**Fig. 4.** Training results of welding defect classification model

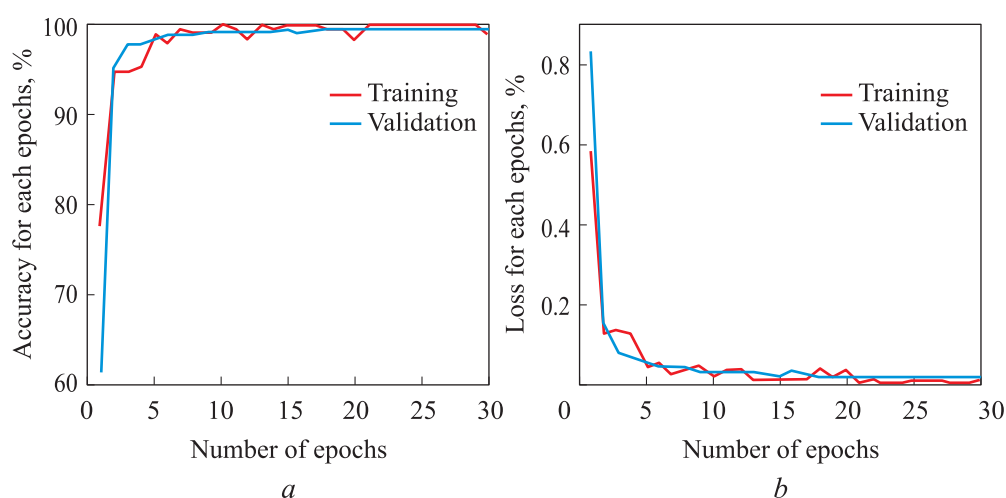


**Fig. 5.** Accuracy of training process (a), loss of training process (b)

The results obtained 99.55 % classification accuracy and 0.45 % classification error. Classification error is the number of classified images incorrectly in the total number of classified images (~ 22 image / 4800 image).

Using the same test data set of welding surface defects with classification models such as Resnet-50 in combination with SVM classifier; Alexnet; Resnet-50 incorporates the Random Forest classifier, we have the results according to Table.

#### Comparison of the classification accuracy of models

Classification Model	Accuracy, %
Resnet-50 + SVM	99.07
Resnet-50 + Random Forest	97.76
Alexnet	99.42
VGG16	99.48
Proposed model in this paper	99.55

Comparing the classification results with the popular convolution neural network models, we find that the proposed classification model in this paper has higher accuracy. The proposed model has a simpler structure, lower computational complexity, and faster training time than compared models. Therefore it can be applied to solve the problem of classifying weld surface defects in real time.

**Conclusion.** In this paper, we present the main types of defects on weld seam. The weld defects image data set was collected and normalized by some

traditional image processing methods. A type of convolutional neural network structure to extract high-level features and classify weld seam defect images is also proposed. Based on previous studies, the parameters of the training process are adjusted to suit the training process of CNN network such as learning speed, parameters of convolution layers, average pooling layers, functions to activate hidden layers, the classification layer and the SGDM algorithm optimize the weight vectors of the layers. Comparing training results and classification of popular models today, we see better classification accuracy of the proposed model and faster training time.

Translated by author

## REFERENCES

- [1] Cary H.B., Helzer S.C. Modern welding technology. New Jersey, Pearson, 2005.
- [2] Primo J. Welding inspection qualifications and testing procedures. PD Honline Course M415 (8PDH). PHD Center, 2012.
- [3] Petcher P.A., Dixon S. Weld defect detection using PPM EMAT generated shear horizontal ultrasound. *NDT E Int.*, 2015, vol. 74, pp. 58–65.  
DOI: <https://doi.org/10.1016/j.ndteint.2015.05.005>
- [4] Zou Y.R., Du D., Chang B.H., et al. Automatic weld defect detection method based on Kalman filtering for real-time radiographic inspection of spiral pipe. *NDT E Int.*, 2015, vol. 72, pp. 1–9. DOI: <https://doi.org/10.1016/j.ndteint.2015.01.002>
- [5] Dzikowski L. Elimination of coil lift off from eddy current measurements of conductivity. *IEEE Trans. Instrum. Meas.*, 2013, vol. 62, no. 12, pp. 3301–3307.  
DOI: <https://doi.org/10.1109/TIM.2013.2272842>
- [6] Kumar G.S., Natarajan U., Ananthan S.S. Vision inspection system for the identification and classification of defects in MIG welding joints. *Int. J. Adv. Manuf. Technol.*, 2011, vol. 61, no. 9-12, pp. 923–933.  
DOI: <https://doi.org/10.1007/s00170-011-3770-z>
- [7] Yan W., Yi S., Peng L., et al. Detection of line weld defects based on multiple thresholds and support vector machine. *NDT E Int.*, 2008, vol. 41, no. 7, pp. 517–524.  
DOI: <https://doi.org/10.1016/j.ndteint.2008.05.004>
- [8] Valavanis I., Kosmopoulos D. Multiclass defect detection and classification in weld radiographic images using geometric and texture features. *Expert Syst. Appl.*, 2010, vol. 37, no. 12, pp. 7606–7614. DOI: <https://doi.org/10.1016/j.eswa.2010.04.082>
- [9] Boaretto N., Centeno T.M. Automated detection of welding defects in pipelines from radiographic images DWDI. *NDT E Int.*, 2017, vol. 86, pp. 7–13.  
DOI: <https://doi.org/10.1016/j.ndteint.2016.11.003>
- [10] Zapata J., Vilar R., Ramon R. Performance evaluation of an automatic inspection system of weld defects in radiographic images based on neuro-classifiers. *Expert Syst. Appl.*, 2011, vol. 38, no. 7, pp. 8812–8824.  
DOI: <https://doi.org/10.1016/j.eswa.2011.01.092>

- [11] Jiang H., Zhao Y., Gao J., et al. Weld defect classification based on texture features and principal component analysis. *Insight Destruct. Test. Cond. Monit.*, 2016, vol. 58, no. 4, pp. 194–200. DOI: <https://doi.org/10.1784/insi.2016.58.4.194>
- [12] Krizhevsky A., Sutskever I., Hinton G.E. ImageNet classification with deep convolutional neural networks. *Adv. Neural Inform. Proc. Syst.*, 2012, vol. 25, pp. 1097–1105.
- [13] Lecun Y., Bengio Y., Hinton G.E. Deep learning. *Nature*, 2015, no. 521, pp. 436–444.
- [14] Sizyakin R.A., Voronin V., Gapon N., et al. Automatic detection of welding defects using the convolutional neural network. *Proc. SPIE*, 2019, no. 11061. DOI: <https://doi.org/10.1117/12.2525643>
- [15] Zhu H., Ge W., Liu Z. Deep learning-based classification of weld surface defects. *Appl. Sc.*, 2019, vol. 9, no. 16, art. 3312. DOI: <https://doi.org/10.3390/app9163312>
- [16] Hou W., Wei Y., Guo J., et al. Automatic detection of welding defects using deep neural network. *J. Phys.: Conf. Ser.*, 2017, vol. 933, no. 012006. DOI: <https://doi.org/10.1088/1742-6596/933/1/012006>
- [17] Riffó V., Lobel H., Mery D. GDXray: the database of X-ray images for nondestructive testing. *J. Nondestruct. Eval.*, 2015, vol. 34, no. 4, art. 42. DOI: <https://doi.org/10.1007/s10921-015-0315-7>
- [18] Hou W., Wei Y., Jin Y., et al. Deep features based on a DCNN model for classifying imbalanced weld flaw types. *Measurement*, 2019, vol. 131, pp. 482–489. DOI: <https://doi.org/10.1016/j.measurement.2018.09.011>
- [19] Yang N., Niu H., Chen L., et al. X-ray weld image classification using improved convolutional neural network. *AIP Conf. Proc.*, 2018, vol. 1995, no. 020035. DOI: <https://doi.org/10.1063/1.5048766>
- [20] Liu B., Zhang X., Gao Z., et al. Weld defect images classification with VGG16-based neural network. In: *Digital TV and Wireless Multimedia Communication*. Springer, 2018, pp. 215–223.
- [21] Golodov V.A., Mittseva A.A. Weld segmentation and defect detection in radiographic images of pipe welds. *Proc. RusAutoCon*, 2019. DOI: <https://doi.org/10.1109/RUSAUTOCON.2019.8867734>
- [22] Khumaidi A., Yuniarno E.M., Purnomo M.H. Welding defect classification based on convolution neural network (CNN) and Gaussian kernel. *Proc. ISITIA*, 2017. DOI: <https://doi.org/10.1109/ISITIA.2017.8124091>

**Gavrilov A.I.** — Cand. Sc. (Eng.), Assoc. Professor, Department of Automatic Control Systems, Bauman Moscow State Technical University (2-ya Baumanskaya ul. 5/1, Moscow, 105005 Russian Federation).

**Do M.Tr.** — Post-Graduate Student, Department of Automatic Control Systems, Bauman Moscow State Technical University (2-ya Baumanskaya ul. 5/1, Moscow, 105005 Russian Federation).

**Please cite this article as:**

Gavrilov A.I., Do M.Tr. Classification of weld defects based on convolution neural network. *Herald of the Bauman Moscow State Technical University, Series Instrument Engineering*, 2021, no. 2 (135), pp. 23–36.

DOI: <https://doi.org/10.18698/0236-3933-2021-2-23-36>



В Издательстве МГТУ им. Н.Э. Баумана  
вышел в свет учебник авторов  
**Е.А. Микрина, Ф.В. Звягина**

**«Введение в механику полета  
и управление космическими аппаратами»**

Представлены основные сведения о технологическом цикле космических полетов, даны примеры практических задач, решаемых в процессе предварительного проектирования и управления полетом космических аппаратов и их группировок.

**По вопросам приобретения обращайтесь:**  
105005, Москва, 2-я Бауманская ул., д. 5, корп. 1  
+7 (499) 263-60-45  
[press@bmstu.ru](mailto:press@bmstu.ru)  
<https://bmstu.press>